Intervals of color mismatch in chromaticity coordinates and in cone-fundamental-based (LMS) space

Fernando Carreño

Departamento de Óptica,

Facultad de Óptica y Optometría, UCM,

C/ Arcos de Jalón 118, Madrid 28037, SPAIN

fcarreno@ucm.es

1 Abstract

We discuss the uncertainties in chromaticity coordinates in the color matching experiment reported by MacAdam [J. Opt. Soc. Am **32**, 247 (1942)]. We also derive the uncertainties in cone-pigments based excitation space. The observer made color matchings by tuning the angle of a Rochon prism. The intervals of color mismatch were obtained using the average value and the standard deviations of the angle settings. We use in this work a rigorous statistical method to derive the probability density functions of chromaticity coordinates assuming a Gaussian distribution for the Rochon prism angle. We also derive the probability density functions of the L-, M-, and S- tristimulus values. We analyze how much the actual probability density functions deviate from the Gaussian. Finally, we determine the bounds of the intervals of color mismatch assuming that the areas of the tails of each probability density function are equal. The so derived intervals are compared to those reported in the original investigation due to MacAdam. We show that color-differences for a certain confidence level cannot be obtained as a simple common scaling factor of the color differences computed for a lower confidence level. The results obtained in LMS space at corneal level exhibit asymmetries between increment and decrement thresholds.

2 Introduction

MacAdam published the results of his pioneering experiment on color-difference thresholds in 1942[1]. In that work color matchings in a two-degree bipartite field were reported for observer Perley G. Nutting (PGN in what follows). A test stimulus was set by the experimenter in one half of the split field. The observer task was to turn a knob that changed the angle (θ) of a Rochon prism. This in turn modified the stimulus in the other half field until a matching between the two fields was established. In the experiment different combinations in pairs of 105 filters were used. The angle θ could be modified at will between 0^0 and 90^0. The instrument was designed in such a way that i) the luminance was kept almost constant, and ii) the locus of possible matches was a straight line in the chromaticity diagram determined by the chromaticity coordinates of each filter pair. This may be called a *guided color matching*, in distinction from a free one where the three tristimulus values could be varied. The 25 color matching ellipses are one of the most widely known results obtained by MacAdam (see Figures 24 to 47 in Ref. [1]). The data for the ellipses are listed in Table III of Ref. [1].

In this work we do not analyze the ellipses, which have been probably over-analyzed, and instead resort to an analysis of a lesser-known part of the experiment in Ref. [1] related to purity matchings and the

corresponding data are listed in Table II of Ref. [1]. We report the results of our analysis in the chromaticity-luminance space which was the one used in Ref. [1]. We also determine the thresholds in LMS tristimulus space.

Standard deviations of matching the purity of selected chromaticities are displayed in Figures 8 to 22 in Ref. [1]. The data are given in Table II of Ref. [1]. The filter pairs can be classified into two groups. In the first group (1), filter number 23 was used. In the second group (2) filter 23 was explicitly factored out. Group 1 can be further divided into two subgroups: in the first subgroup 17 filter pairs were used to produce chromaticities with dominant wavelength (group 1A), and in the second one 9 filter pairs were used to produce chromaticities with complementary wavelength (group 1B). The 9 filter pairs in group 2 were used to produce chromaticities close to the spectral locus. A total of 230 color centers were analyzed in the first part of the experiment reported in Ref. [1]. The chromaticity coordinates of the color centers of the ellipses listed in Table III of Ref. [1] have been plotted in Fig. 1(d) for completeness.

The chromaticities of the color centers are indicated by crosses in Fig. 1(a)-(c). The straight lines joining the chromaticities of the different filter pairs have been plotted as well. The

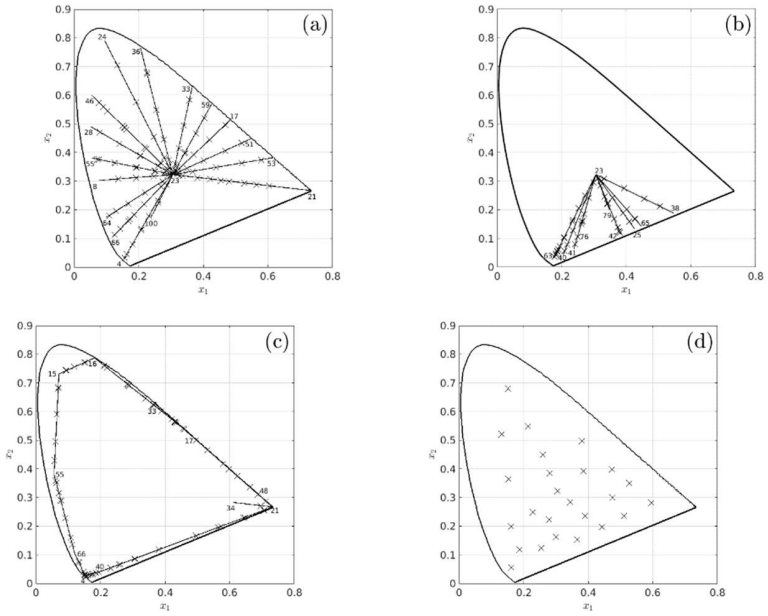

Figure 1: Chromaticity diagram of the CIE1931 standard observer together with straight lines defined by the chromaticities of each filter pair. The data used have been extracted from Table II in Ref. [1]. The crosses on the straight lines indicate the average chromaticities of the different color centers analyzed. (a) Filter pairs with dominant wavelength (group 1A). A total of 17 filter pairs are in this group. (b) Filter pairs with complementary wavelength (group 1B). A total of 9 filter pairs are in this group. (c) The rest of filter pairs (group 2). A total of 9 filter pairs are in this group. (d) Color centers of the ellipses listed in Table III of Ref. [1].

One of the filters provided a given chromatic stimulus when the angle was 0^0. The other filter of the filter pair at 90^0 was chosen to provide different guided matchings along the straight line joining the chromaticities of each filter pair. The dominant/complementary wavelength was determined for the different filter pairs in group 1.

The tristimulus values of the mixture of the lights transmitted by a given filter pair depend on the angle setting θ and read

$$X_j = X_{j,u}\sin^2(\theta) + X_{j,v}\cos^2(\theta) (j = 1,2,3). \quad (1)$$

We assume that X_1=X, X_2=Y, and X_3=Z. Equation (1) is the same as Eqs. (2)-(4) in page 255 of Ref. [1]. We prefer the use of subscripts because it makes the notation more compact. The additional subindex $u(v)$ in Eq. (1) allows us to indicate what the filter is when the angle is $90^0(0^0)$. The tristimulus values of each filter are given in Table I of Ref. [1]. The average value (θ_0) and the standard deviation (σ_θ) of N=50 matchings made by observer PGN were written down for different combinations of filter pairs (see Table II in Ref. [1]). It should be noted that the total number of matchings carried out for the 230 color centers listed in Table II of Ref. [1] adds up to 11500, which reveals the magnitude of the experimental task performed. The tristimulus values of the filters listed in Table I of Ref. [1] were computed using the color matching functions of CIE1931 standard observer. The identity of the color matching functions of observer PGN to those of the CIE1931 standard observer was assumed in Ref. [1].

A color stimulus can be specified by its chromaticity coordinates and luminance. The chromaticity coordinates are given by

$$x_j = X_j / \sum_{k=1}^{3} X_k \ (j = 1,2). \quad (2)$$

The color mismatch in Ref. [1] was only attributed to the uncertainty in the angle settings. The uncertainties arising from fluctuations of the tristimulus values of the filters were neglected. We also follow this assumption when deriving the experimental errors of magnitudes x_j (j=1,2).

The conventional approach to determine the uncertainty of x_j is based on the calculation of the following magnitude (see Ref. [2])

$$\sigma^2(x_j) = \left|\frac{\partial x_j}{\partial \theta}\right|^2 \sigma_\theta^2 (j = 1,2). \quad (3)$$

The average chromaticity coordinates ($\overline{x_j}$) are computed by using Eq. (2) for the average angle (θ_0). The associated standard deviations ($\sigma(x_j)$) are derived from Eq. (3). This procedure will produce a symmetric interval of color mismatch, i.e., $\left[\overline{x_j} - \sigma(x_j), \overline{x_j} + \sigma(x_j)\right]$. The standard deviation reads

$$\sigma(x_j) = \sin(2\theta_0) \times \left|\frac{X_{j,u}X_v - X_{j,v}X_u}{((X_v - X_u)\times co\ ^2(\theta) + X_u)^2}\right| \sigma_\theta (j = 1,2), \quad (4)$$

where $X_u = \sum_{k=1}^{3} X_{k,u}$ and $X_v = \sum_{k=1}^{3} X_{k,v}$.

The use of Eq. (4) is justified as far as the function which defines x_j as a function of θ is linear as it was the case considered in Ref. [2]. However, the function in Eq. (1) involves quadratic terms in trigonometric functions and, in addition, the chromaticity coordinates derived from Eq. (2) arise also from a nonlinear transformation, and they could produce a significant departure of the uncertainty in x_j when derived using Eq. (4) from the actual uncertainty as derived from statistical theory. In other words, instead of using Eq. (4), in this work we resort to perform a rigorous statistical analysis of the problem. This will allow us to determine to what extent the conventional approach can be used when applied to a certain experimental situation.

We used statistical theory to derive the intervals of color mismatch in tristimulus space in our previous work [3]. We determined the probability density function (PDF) of the three tristimulus values. The formalism was applied to the experimental data randomly selected from Table III of Ref. [1]. The intervals of color mismatch derived by us exhibit asymmetries. Those based on the conventional approach are symmetrical in nature. Our previous work [3] closely follows Ref. [4]. The purpose of the current work is to determine the color-differences in chromaticity-luminance space [(x_1,x_2,X_2)]. In Section 3 we derive the PDFs for the chromaticity coordinates. The new PDFs differ from the ones obtained for tristimulus values, although they also exhibit asymmetries which make them to depart from a Gaussian PDF. The numerical results are presented in Section 4. Section 5 is devoted to present the PDFs of the tristimulus values in LMS

space at a corneal level. Section 6 summarizes the main conclusions.

3 Derivation of probability density functions of chromaticity coordinates

Let us consider that the angle setting (θ) behaves as a Gaussian with mean value θ_0 and standard deviation σ_θ, i.e., θ is a $N(\theta_0,\sigma_\theta)$. The associated probability density function (PDF) reads

$$f(\theta) = \frac{1}{\sqrt{2\pi\sigma^2}} e^{\frac{-(\theta-\theta_0)^2}{2\sigma_\theta^2}}. \quad (5)$$

We want to draw the attention to the fact that a Gaussian PDF has a null asymmetry (As=0) while the kurtosis parameter (K) is equal to 3 (see Ref. [5]).

In view of the fact that θ is a random variable, any function of θ, let's say $g(\theta)$, is a new random variable [5]. This obviously applies to the case of chromaticity coordinates given in Eq. (2). This problem is addressed in this work by using the standard technique described in detail in Ref. [5], provided that the inverse function exists, as it is the case.

The chromaticity coordinates as a function of the angle θ read

$$x_j = \frac{(X_{j,u}-X_{j,v})\times cos^2(\theta)+X_{j,u}}{(X_u-X_v)\times cos^2(\theta)+X_u} (j = 1,2), \quad (6)$$

where $X_u = \sum_{j=1}^{3} X_{j,u}$ and $X_v = \sum_{j=1}^{3} X_{j,v}$. Equation (6) can be inverted to obtain $\theta = \theta(x_j)$ $(j = 1,2)$. In view of that the new PDF $\hat{g}(x_j)$ should read as

$$\hat{g}(x_j) = g_N e^{\frac{-1}{2\sigma_\theta^2}[\theta_0-\theta(x_j)]^2} \left|\frac{d\theta(x_j)}{dx_j}\right| (j = 1,2), \quad (7)$$

where the second term inside the absolute value sign accounts for the Jacobian of the inverse function $\theta(x_j)$. The explicit expression for the Jacobian reads

$$\left|\frac{d\theta(x_j)}{dx_j}\right| = \left|\frac{X_v X_{ju} - X_u X_{jv}}{\left[(X_{ju}-X_{jv}+x_j[X_v-X_u])^2 \times (X_{ju}-x_j X_u)\times(-X_{jv}+x_j X_v)\right]^{1/2}}\right| (j = 1,2), \quad (8)$$

The Jacobian given in Eq. (8) is not a constant as it would be in the case of a linear transformation, and we foresee that this is the origin of the deviations found in this work. Note that Eq. (8) strongly differs from the Jacobian for the PDFs of the tristimulus values (see Eq. (5) in Ref. [3]). Finally, g_N in Eq. (7) is a constant that should be computed to guarantee the normalization of the PDF, i.e., that the following condition holds

$$\int_{x_{j,min}}^{x_{j,max}} \hat{g}(x_j) dx_j = 1 (j = 1,2), \quad (9)$$

where $x_{j,min}=\min(x_{j,u},x_{j,v})$ and $x_{j,max}=\max(x_{j,u},x_{j,v})$.

We compute the mean value of magnitudes x_j, the second, third and fourth moments centered around the mean value for the new PDFs [$\hat{g}(x_j)$] according to the following standard formulas:

$$\begin{aligned}
&\langle x_j \rangle = \int_{x_{j,min}}^{x_{j,max}} x_j\, \hat{g}(x_j) dx_j (j = 1,2),\\
&\langle E_2(x_j) \rangle = \int_{x_{j,min}}^{x_{j,max}} (x_j - \langle x_j \rangle)^2\, \hat{g}(x_j) dx_j (j = 1,2),\\
&\langle E_3(x_j) \rangle = \int_{x_{j,min}}^{x_{j,max}} (x_j - \langle x_j \rangle)^3\, \hat{g}(x_j) dx_j (j = 1,2),
\end{aligned} \quad (10)$$

$$\langle \mathrm{E}_4(x_\mathrm{j})\rangle = \int_{x_{\mathrm{j,min}}}^{x_{\mathrm{j,max}}} (x_\mathrm{j} - \langle x_\mathrm{j}\rangle)^4\, \hat{\mathrm{g}}(x_\mathrm{j})\mathrm{d}x_\mathrm{j} (\mathrm{j} = 1{,}2).$$

Quantities $\langle \mathrm{E}_2(x_\mathrm{j})\rangle$, $\langle \mathrm{E}_3(x_\mathrm{j})\rangle$ and $\langle \mathrm{E}_4(x_\mathrm{j})\rangle$ in Eq. (10) are central moments (see for example Section 5-4 in Ref. [5]).

The standard deviation is $\hat{\sigma}(x_j) = \left(\mathrm{E}_2(x_\mathrm{j})\right)^{1/2}$, while the asymmetry ($As$) and kurtosis ($K$) parameters read

$$As(x_\mathrm{j}) = \frac{\mathrm{E}_3(x_\mathrm{j})}{\left(\hat{\sigma}(x_\mathrm{j})\right)^3} (\mathrm{j} = 1{,}2),$$

$$K(x_\mathrm{j}) = \frac{\mathrm{E}_4(x_\mathrm{j})}{\left(\hat{\sigma}(x_\mathrm{j})\right)^4} (\mathrm{j} = 1{,}2). \qquad (11)$$

The values of the standard deviation of the chromaticity coordinates obtained using Eq. (10) should be compared with those derived from Eq. (2). In addition, the results obtained for the asymmetry and kurtosis parameters should be compared with those of a Gaussian function. These comparisons will allow us to check the severity of the nonlinear transformations between the angle settings and the chromaticity coordinates. Note that for given filter pair U_a and V_a, and the corresponding values (θ_0, σ_θ), the asymmetry and kurtosis parameters associated to the chromaticity coordinates should differ from those for the tristimulus values, the reason being that here we are considering an additional transformation from (X_1,X_2,X_3) space to (x_1,x_2,X_2) space.

3.1 Numerical results

An interesting aspect investigated in Ref. [1] is the color discrimination in purity. Let us consider a fixed filter pair either in group 1 or group 2 in Fig. 1(a)-(c). Several stimuli were presented in the fixed field corresponding to different chromaticities. The average angle settings and their standard deviations are provided in Table II of Ref. [1]. The results are displayed in Figs. 8-22 of Ref. [1].

The results of applying our statistical procedure to the case of filters 4(0^0) and 23 (90^0) (see upper part of left column in page 258 of Ref. [1]) are listed in Table 1. This filter pair belongs to group 1A and is in no way exceptional among the 35 filter pairs. The numerical integration indicated in Eqs. (9)-(10) was made using standard quadrature functions [6, 7]. The tolerance to compute the integrals in Eq. (9) was set to 10^{-8}.

θ_0	σ_θ	$As(x_1)$	$As(x_2)$	$K(x_1)$	$K(x_2)$	$\lvert As(X_i)\rvert$	$\lvert K(X_i)\rvert$	x_{1M}	x_{2M}
83.8	0.239	-0.0621	-0.0621	2.9988	2.9988	0.1138	3.0170	0.286	0.286
79.1	0.256	0.0106	0.0106	2.9969	2.9969	0.0670	3.0057	0.259	0.233
79.1	0.230	0.0095	0.0095	2.9975	2.9975	0.0602	3.0046	0.259	0.233
74.1	0.247	0.0397	0.0397	3.0017	3.0017	0.0417	3.0020	0.230	0.177
69.0	0.382	0.0768	0.0768	3.0098	3.0098	0.0444	3.0019	0.208	0.135

68.5	0.304	0.0616	0.0616	3.0064	3.0064	0.0341	3.0011	0.206	0.131
58.4	0.335	0.0676	0.0676	3.0084	3.0084	0.0177	2.9999	0.180	0.081
42.1	0.477	0.0824	0.0824	3.0125	3.0125	0.0051	2.9989	0.162	0.045
25.1	0.563	0.0988	0.0988	3.0164	3.0164	0.0491	3.0017	0.155	0.031

Table 1: The first and second columns provide the average angles and standard deviations obtained with filter pair 4/23 ($0^0/90^0$) of group 1A for the different stimuli provided in Table II of Ref. [1]. The third and fourth columns provide the values of asymmetry coefficients of the PDFS of the chromaticity coordinates, while the fifth and sixth columns provide the values of kurtosis coefficients of the PDFS of the chromaticity coordinates. The seventh and eighth columns give the absolute values of asymmetry and kurtosis coefficients of the PDFS of the tristimulus values. The ninth and tenth columns reproduce the chromaticity coordinates given in Table II of Ref. [1].

The inspection of Table 1 reveals that the departure from zero of the asymmetry coefficients strongly depends on the average angle (θ_0) considered. It takes negative values when θ_0 is close to 90^0, and it changes its sign and magnitude as θ_0 approaches 0^0. The kurtosis parameter is below(above) the value of 3 when θ_0 is close to $90^0(0^0)$. These results are not unexpected in view of the nonlinear character of Eq. (1) and the additional projective transformation from tristimulus values to chromaticity coordinates of Eq. (2) which is also a nonlinear mapping as indicated in Eq. (8). In any case the results obtained for both the asymmetry and kurtosis parameters for the PDFs of the chromaticity coordinates differ from those of a Gaussian, and this will, in turn, produce deviations of the intervals of color mismatch in chromaticity coordinates as we will show later in this work. It is worth noting that the asymmetries ($As(x_j)$) and kurtosis ($K(x_j)$) listed in Table 1 take similar values to the ones obtained in Ref. [4] (see Table 2 in Ref. [4]) where we analyzed the experimental data reported in Ref. [8].

We also computed the asymmetry and kurtosis parameters for the PDFs of the tristimulus values. The absolute values are listed in seventh and eighth columns of Table 1. They differ from those obtained for the chromaticity coordinates. This is an indication of the influence on the PDFs of the nonlinear transformation from tristimulus space to chromaticity-luminance space.

The PDFs of the chromaticity coordinates obtained for the filter pair 4/23 ($0^0/90^0$) in the case with θ_0=25.1^0 and σ_θ=0.563^0 are displayed in Figure 2. We choose this angle setting because it is the one which exhibits the highest degree of asymmetry for chromaticity coordinates (see Table 1). The mean values $(\langle x_j \rangle)$ are indicated with a star in each panel. In addition, we have plotted with open circles the points which are apart from $\langle x_j \rangle$ by $\hat{\sigma}(x_j)$. An inspection of Fig. 2 shows that the open circles are not symmetrically located around the corresponding mean values.

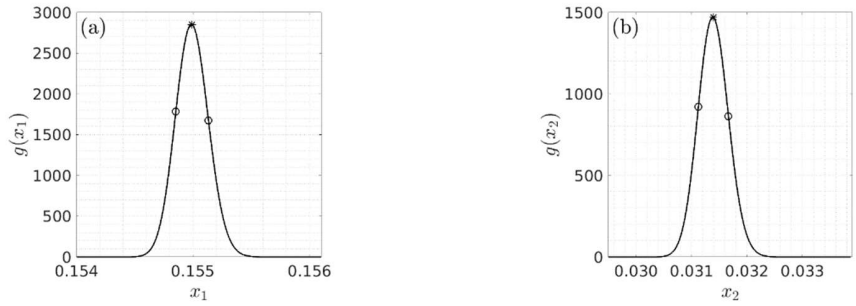

Figure 2: PDFs of the chromaticity coordinates obtained with filter pair 4/23 (0^0/90^0) in group 1A, average angle θ_0=25.1^0 and σ_θ=0.563^0. Stars are used to indicate the mean value $\langle x_j \rangle$, whereas open circles indicate the positions of the points apart from the mean value by $\hat{\sigma}(x_j)$.

We performed several tests of Gaussianity on the PDFs of the chromaticity coordinates. Each chromaticity coordinate x_j was sampled around the point $\langle x_j \rangle$. The sampling interval was sufficiently wide to ensure that the values of functions $\hat{g}(x_j)$ at the ends of the interval were in the order for 10^{+14} lesser than the peak value. A publicly available Matlab script [9] has been used to test the Gaussianity of functions $\hat{g}(x_j)$. Nine of the ten tests yielded zero as a result for the 230 color centers and the PDFs of the two chromaticity coordinates, which means that the PDFs can be considered as non- normal distributions. The only test that yields a value of 1 (normal) was the Cramer-Von Mises with a p-value of ∞. This indicates that this test is not reliable.

Let us analyze how close are the values of the chromaticity coordinates determined by us $(\langle x_j \rangle)$to the ones given in Table II of Ref. [1]. We performed linear fits between our data ($\langle x_j \rangle$) and those listed in columns nine and ten in Table 1. The results are shown in Fig. 3. The slopes of the fittings differ from unity in the third decimal place. The intercepts differ from zero in the fourth decimal place. The R-squared correlation coefficients differ from unity in the fifth decimal place. Note that the chromaticity coordinates given in Ref. [1] were obtained using a slide rule which was specially designed for that research (see page 256 and Fig. 7 in page 257 of Ref. [1] for more details), and they were provided with three decimal places. However, our computation has been made with a modern computer using floating point arithmetic, which is more accurate.

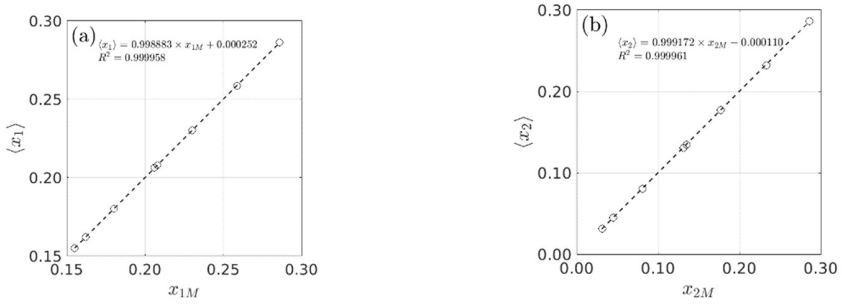

Figure 3: Average chromaticity coordinates ($\langle x_j \rangle$) obtained using Eq. (10) for filter pair 4/23 at 0^0/90^0 in group 1A, average angle θ_0=25.1^0 and σ_θ=0.563^0, versus the chromaticity coordinates (x_{jM}) listed in Table 1 (obtained from Table II of Ref. [1]).

The tristimulus value $\langle X_2 \rangle$ of the color centers listed in Table 1 are within the interval [0.00283, 0.00294]. The average value is $\langle\langle X_2 \rangle\rangle = 0.00291$ and the standard deviation is $\sigma_{X_2} = 0.00004$. The coefficient of variation is $\sigma_{X_2}/\langle\langle X_2 \rangle\rangle = 1.34\%$ for this filter pair. Figure 4 shows the values of $\langle X_2 \rangle$ obtained for the 230 color centers considered in Table II of Ref. [1]. The average value and the coefficient of variation when considering all the color centers are $\langle\langle X_2 \rangle\rangle = 0.00284$ and 3.13 % respectively. The fact that some points fall outside the 1σ uncertainty interval is an indication of the experimental difficulty encountered in designing the filters used in the experiment of Ref. [1].

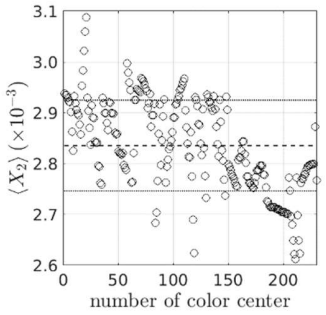

Figure 4: Values of tristimulus value $\langle X_2 \rangle$ for the 230 color centers considered in Table II of Ref. [1]. The horizontal dashed line indicates the mean value $\langle\langle X_2 \rangle\rangle = 0.00284$ obtained for all the color centers, while the horizontal dotted lines indicate the corresponding ±1σ uncertainty interval.

Similar results to those displayed in Table 1 and Figs. 1-3 are obtained when considering other filter pairs listed in Table II of Ref. [1]. We omit them to avoid this paper to be an excessively long one.

4 Interval of color mismatch in chromaticity coordinates

We have indicated after Eq. (3) that when we use the conventional approach, the uncertainty interval for a particular chromaticity coordinate is $\left[\,\overline{x_{\mathrm{j}}} - \sigma(x_{\mathrm{j}}), \overline{x_{\mathrm{j}}} + \sigma(x_{\mathrm{j}})\,\right] (j = 1,2)$. However, this procedure does not capture the nonsymmetrical nature of the PDF, as it has been illustrated previously in this work (see Table 1 and Fig. 2).

Let us make a choice for the confidence level α to determine the interval of color mismatch, or color uncertainty interval. Usual values for α are 0.32, 0.16 or 0.05. It means that (1−α)×100 of the settings of a given magnitude will lie within the uncertainty interval.

We described in Ref. [3] two methods to derive the interval of color mismatch. We are going to use method 2 which is briefly summarized as follows: let $x_{\mathrm{j,L}}^{(2)}$ and $x_{\mathrm{j,U}}^{(2)}$ be the lower and upper bounds of the interval corresponding to the chromaticity coordinate $x_{\mathrm{j}} (\mathrm{j} = 1,2)$, i.e., $\mathrm{I}_{\mathrm{j}}^{(2)} = \left[x_{\mathrm{j,L}}^{(2)}, x_{\mathrm{j,U}}^{(2)}\right]$. This interval should satisfy the following identity

$$\int_{x_{\mathrm{j,L}}^{(2)}}^{x_{\mathrm{j,U}}^{(2)}} \hat{\mathrm{g}}(x_{\mathrm{j}})\mathrm{d}x_{\mathrm{j}} = (1 - \alpha)(\mathrm{j} = 1,2). \qquad (12)$$

The lower and upper bounds of such interval can be determined by assuming that the areas of the tails of the PDFs are equal, i.e., the following conditions hold

$$\int_{x_{\mathrm{j,min}}}^{x_{\mathrm{j,L}}^{(2)}} \hat{\mathrm{g}}(x_{\mathrm{j}})\mathrm{d}x_{\mathrm{j}} = \frac{\alpha}{2}(\mathrm{j} = 1,2),$$

(13)

$$\int_{x_{\mathrm{j,U}}^{(2)}}^{x_{\mathrm{j,max}}} \hat{\mathrm{g}}(x_{\mathrm{j}})\mathrm{d}x_{\mathrm{j}} = \frac{\alpha}{2}(\mathrm{j} = 1{,}2).$$

Note that we do not make any *a priori* assumption concerning the symmetry of the interval $\mathrm{I}_{\mathrm{j}}^{(2)}$around $\langle x_j \rangle$.

The values for $x_{\mathrm{j,L}}^{(2)}$and $x_{\mathrm{j,U}}^{(2)}$ are determined by numerically solving the quadratures indicated in Eq. (13). In the practical calculation an iterative algorithm is used to determine both $x_{\mathrm{j,L}}^{(2)}$and $x_{\mathrm{j,U}}^{(2)}$, and the iteration is halted when the numerical value of the integrals in Eq. (13) differs from the prescribed value indicated in the right-hand sides of Eq. (13) by 10^{-8}.

Note that the uncertainty region around each color center (D_c) will generally be a rectangle, and it is determined by $D_c \equiv \mathrm{I}_1^{(2)} \times \mathrm{I}_2^{(2)} = \left[x_{1,\mathrm{L}}^{(2)}, x_{1,\mathrm{U}}^{(2)}\right] \times \left[x_{2,\mathrm{L}}^{(2)}, x_{2,\mathrm{U}}^{(2)}\right]$.

Finally, the color-differences in chromaticity coordinates are given by the euclidean distance from the mean value $\left(\langle x_{\mathrm{j}} \rangle\right)$ to the upper and lower limits of the two sub-intervals and read

$$ds_{+}^{(2)} = \left[\sum_{j=1}^{2}\left(x_{j,U}^{(2)} - \langle x_j \rangle\right)^2\right]^{1/2},$$

$$ds_{-}^{(2)} = \left[\sum_{j=1}^{2}\left(x_{j,L}^{(2)} - \langle x_j \rangle\right)^2\right]^{1/2}, \tag{14}$$

when the slope of the straight line joining the filters is positive, and

$$ds_{+}^{(2)} = \left[\left(x_{1,L}^{(2)} - \langle x_j \rangle\right)^2 + \left(x_{2,U}^{(2)} - \langle x_j \rangle\right)^2\right]^{1/2},$$

$$ds_{-}^{(2)} = \left[\left(x_{1,U}^{(2)} - \langle x_j \rangle\right)^2 + \left(x_{2,L}^{(2)} - \langle x_j \rangle\right)^2\right]^{1/2}, \tag{15}$$

when the slope of the straight line joining the filters is negative. Note that both $ds_{+}^{(2)}$and $ds_{-}^{(2)}$ depend on the choice made for α.

The use of Eq. (14) or alternatively Eq. (15) is based on the sign of the slope of the line joining the chromaticities of the filter pair. Figure 5 displays the uncertainty region D_c for the filter pair 4 and 23 of group 1A for θ_0=25.1^0 and σ_θ=0.563^0. Two of the four corners of each uncertainty rectangle were considered in Ref. [2]. The points considered were those through which the line joining the chromaticities of the filter pair passed while the other two points were discarded. We will follow this prescription in what follows.

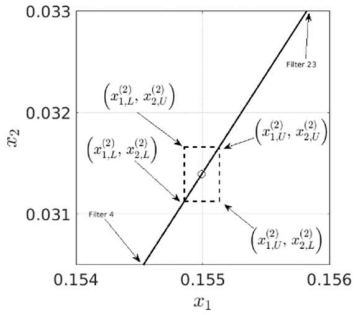

Figure 5: 2D region of uncertainty (D_c) in the chromaticity diagram for the first filter pair in group 1A in Table II in Ref. [1]. The average chromaticity is indicated with an open symbol. The dashed lines indicate the limits of D_c in the case α=0.32. The straight line joins the chromaticities of the filter pair used. The filters used are 4 at 0^0 and 23 at 90^0 for θ_0=25.1^0 and σ_θ=0.563^0.

The distance obtained by using Eq. (2) reads as

$$ds_c = \left(\sum_{j=1}^{2}\left[\sigma(x_j)\right]^2\right)^{1/2}, \tag{16}$$

where the subscript c is used to indicate the conventional approach and $\sigma(x_j)$ is given by Eq. (4).

Distances $ds_{\pm}^{(2)}$ and ds_c could be compared among them in the case with α=0.32 to get an idea about the discrepancies between the two approaches.

The distances $ds_{\pm}^{(2)}$ and ds_c given in Eqs. (14)-(15) are an approximation because they do not consider the changes in luminance. The changes in luminance can be added to the color-difference by taking into account the PDF for X_2, $g(X_2)$ (see Eq. (5) in Ref. [3]). We should determine the upper ($X_{2,U}^{(2)}$) and lower ($X_{2,L}^{(2)}$) limits of the interval for X_2 by imposing a condition equivalent to Eq. (12) but using $g(X_2)$. The full color-difference should read

$$ds_{+}^{(3)} = \left[\sum_{j=1}^{2}\left(x_{j,U}^{(2)} - \langle x_j\rangle\right)^2 + \left(X_{2,U}^{(2)} - \langle X_2\rangle\right)^2\right]^{1/2},$$

$$ds_{-}^{(3)} = \left[\sum_{j=1}^{2}\left(x_{j,L}^{(2)} - \langle x_j\rangle\right)^2 + \left(X_{2,L}^{(2)} - \langle X_2\rangle\right)^2\right]^{1/2}, \tag{17}$$

when the slope of the straight line joining the filters is positive, and

$$ds_{+}^{(3)} = \left[\left(x_{1,L}^{(2)} - \langle x_j\rangle\right)^2 + \left(x_{2,U}^{(2)} - \langle x_j\rangle\right)^2 + \left(X_{2,U}^{(2)} - \langle X_2\rangle\right)^2\right]^{1/2},$$

$$ds_{-}^{(3)} = \left[\left(x_{1,U}^{(2)} - \langle x_j\rangle\right)^2 + \left(x_{2,L}^{(2)} - \langle x_j\rangle\right)^2 + \left(X_{2,L}^{(2)} - \langle X_2\rangle\right)^2\right]^{1/2}, \tag{18}$$

when the slope of the straight line joining the filters is negative.

The color-difference computed in the conventional way should read

$$ds_c^{(3)} = \left(\sum_{j=1}^{2}\left[\sigma(x_j)\right]^2 + \left[\sigma(X_2)\right]^2\right)^{1/2}, \quad (19)$$

where $\sigma(X_2)$ is determined using Eq. (2) of Ref. [3].

4.1 Numerical results

The Euclidean color-differences given in Eq. (14)-(15) and Eq. (16) have been computed for the filter pair used to produce Table 1. The results are displayed in Fig. 6. We can conclude by inspecting Fig. 6(a) that the conventional approach fairly reproduces the standard deviations provided in Table II in Ref. [1]. The closeness among the two sets of data is an indication of the accuracy of the slide rule used in Ref. [1] to derive color-differences. The data in Fig. 6(a) should be compared to those in Fig. 6(b) because they are obtained for the same value of α. An inspection of Fig. 6(a)-(b) reveals that the conventional approach based on the use of Eq. (15) produces similar values for the color-differences for all the average angles considered in Table 1. The asymmetries of color-differences become evident for the lowest value of α [see panel 6(d)].

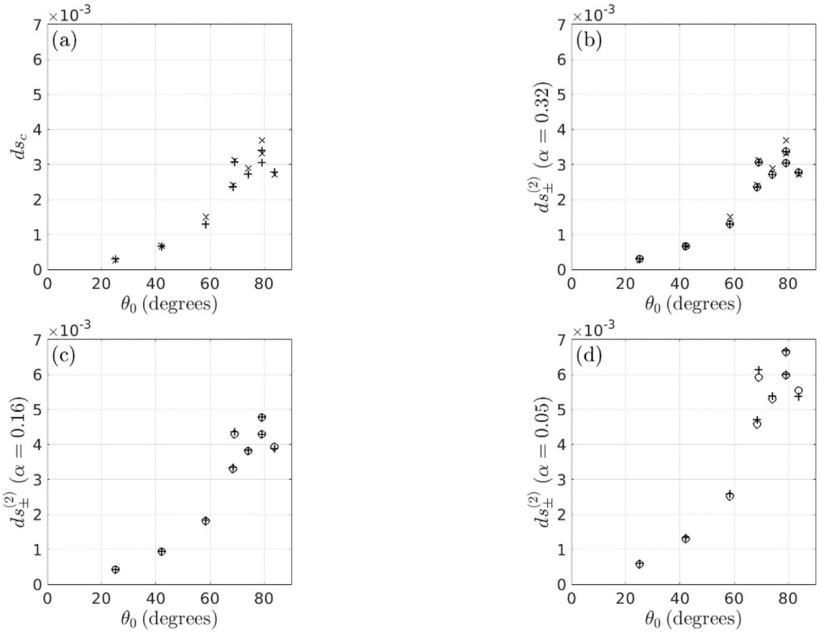

Figure 6: Color-differences between the average chromaticities and the points at the extremes of the uncertainty intervals. (a) Using the conventional procedure given by Eq. (15). In panels (b)-(d) the + symbols are used to designate $ds_+^{(2)}$ distances and the o symbols to designate $ds_-^{(2)}$ distances. In panels (a)-(b) the × symbols denote the standard deviations provided in Ref. [1]. The filters used are 4 at 0^0 and 23 at 90^0 of group 1A. The dominant wavelength of the stimuli produced with this filter pair is 455 nm.

A measure of the magnitude of the asymmetries in color differences can be obtained by the quotient of the distances obtained for α=0.05 and the corresponding distances for α=0.32, i.e., we compute

$$Q_{\pm} = \frac{ds_{\pm}^{(2)}(\alpha=0.05)}{ds_{\pm}^{(2)}(\alpha=0.32}. \quad (20)$$

We know that for a Gaussian variate the interval of uncertainty for α=0.32 has a half-width of one standard deviation (±1σ) centered on the mean value, whereas the uncertainty interval for α=0.05 has a half-

width of ±1.96σ. The results obtained for the 230 color centers of the different groups of filter pairs are shown in Fig. 7(a)-(c). The horizontal axis in Fig. 7 represents the Euclidean distance (d_w) from the average chromaticity of each color center ($\langle x_1 \rangle, \langle x_2 \rangle$) to the chromaticity provided by filter 23 ($\langle x_{1A} \rangle, \langle x_{2A} \rangle$). The latter point was considered as the white point in Ref. [1] when determining the excitation purity of the different stimuli. In all panels the horizontal dashed line corresponds to the value of 1.96. The inspection of Fig. 7 reveals that for values of d_w close/far to the white point the asymmetries are enhanced whereas for intermediate values the cloud of points is close to the horizontal line. This instead means that there is no a clear rule to obtain the color-differences for α =0.05 as a simple common scaling factor of the color differences for α=0.32.

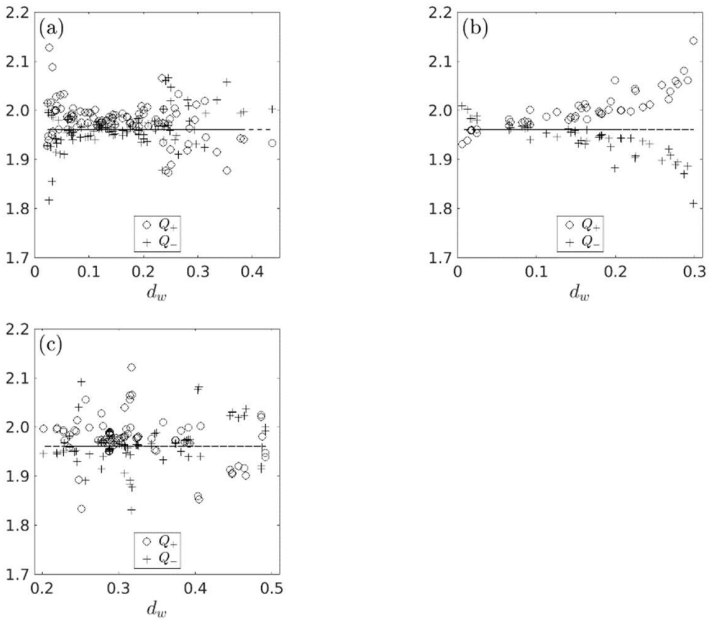

Figure 7: Ratios between the distances obtained for α =0.05 and those for α=0.32 versus the Euclidean distance d_w. (a) Filter pairs in group 1A. (b) Filter pairs in group 1B. (c) Filter pairs in group 2. The horizontal dashed line corresponds to the value 1.96.

The asymmetries of color-differences obtained in this work are in the range of the ones found in Ref. [4] (see Fig. 3 in Ref. [4]). However, note that in Ref. [4] we used Method 1 as in Ref. [3] while in this work we have determined the intervals of color mismatch applying Method 2 from Ref. [3].

Let us consider the influence of luminance on color-differences. We plot the ratio of the distance obtained using Eq. (14) and Eq. (15) and the distance computed using Eq. (17) and Eq. (18). The results obtained for the case of considering the filter pair 4/23 are shown in Fig. 8. The closeness of the quotients to unity is an indication that luminance changes have little effect on color-differences. Similar results are obtained for other filter pairs in Table II of Ref. [1].

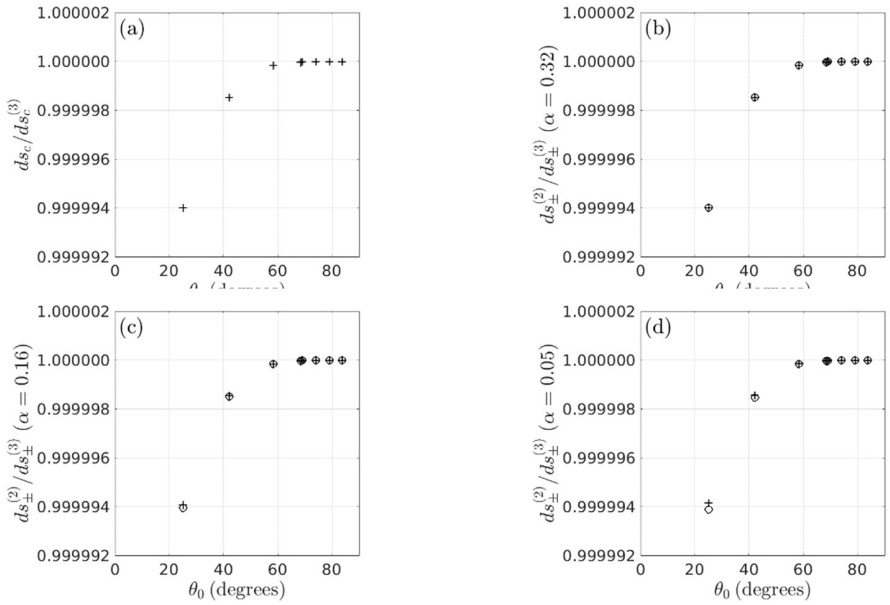

Figure 8: Ratio between color-differences obtained by the two methods: (a) conventional approach $\left(ds_c/ds_c^{(3)}\right)$, and (b)-(d) our approach $\left(ds_\pm^{(2)}/ds_\pm^{(3)}\right)$. The filters used are 4 at 0^0 and 23 at 90^0 of group 1A.

We will close this Section with a final remark concerning the use of Method 1 of Ref. [3] to obtain the intervals of color mismatch. We showed in Ref. [3] that the use of a different criterion (labelled as Method 1) to determine the intervals results in obtaining larger asymmetries than those obtained by Method 2. We also stated that the choice of one method over the other should be an experimental issue. We have made the same computations as the ones presented in this work while using Method 1, and we conclude that Method 1 of Ref. [3] always predict larger asymmetries for color-differences in chromaticity coordinates than those obtained when using Method 2. The origin of these differences arises from the way in which the interval of color mismatch is split: in Method 1 the uncertainty interval is assumed to be given by $I_j^{(1)} = \left[x_{\mathrm{j,L}}^{(1)}, \langle x_\mathrm{j}\rangle\right] \cup \left[\langle x_j\rangle, x_{\mathrm{j,U}}^{(1)}\right]$. In making the previous split of the interval $I_j^{(1)}$ we assume that the proportion 1−α of random samples of fixed size will produce a confidence interval that contain $\langle x_\mathrm{j}\rangle$ which is equally likely to be in the lower or the upper subinterval.

5 Probability density functions and intervals of color-mismatch in L-, M-, S- space

In this Section we present the results of applying our methodology to derive the PDFs and the intervals of color-mismatch in LMS space. The sensitivities of the cones are represented by the fundamentals derived by Smith and Pokorny [10]. The transformation from tristimulus space of the CIE1931 to LMS values is performed through a matrix given by

$$\begin{pmatrix} H_1 \\ H_2 \\ H_3 \end{pmatrix} = \begin{pmatrix} a_{11} & a_{12} & a_{13} \\ a_{21} & a_{22} & a_{23} \\ a_{31} & a_{32} & a_{33} \end{pmatrix} \begin{pmatrix} X_1 \\ X_2 \\ X_3 \end{pmatrix} = \begin{pmatrix} 0.15514 & 0.54321 & -0.03286 \\ -0.15514 & 0.45684 & 0.03286 \\ 0 & 0 & 0.00801 \end{pmatrix} \begin{pmatrix} X_1 \\ X_2 \\ X_3 \end{pmatrix}. \quad (21)$$

We assume that H_1=L, H_2=M, and H_3=S. We prefer the use of subscripts because it makes the notation more compact. The matrix given in Eq. (21) is like the one considered in Refs. [11-12] with H_j (j=1,2,3) values scaled in trolands units. When making use of Eq. (21) the small differences between the CIE1931 observer and the modifications to it by Judd are neglected. A similar approach has been used in Ref. [12].

Let us obtain the H_j values of the stimuli listed in Table II of Ref. [1]. The values of H_j as a function of the angle θ read

$$\theta(H_j) = cos^{-1}\left(\sqrt{\frac{H_j - A_{0j}}{B_{oj}}}\right) (j = 1,2,3), \quad (22)$$

where the constants A_{oj} and B_{oj} read

$$B_{0j} = \sum_{k=1}^{3} a_{jk}\,(X_{kv} - X_{ku})\ (j = 1,2,3), \quad (23)$$

$$A_{0j} = \sum_{k=1}^{3} a_{jk}\,X_{ku} (j = 1,2,3).$$

In view of the previous equations the PDF of H_j, $\tilde{g}(H_j)$, should read as

$$\tilde{g}(H_j) = g_N e^{\frac{-1}{2\sigma_\theta^2}[\theta_0 - \theta(H_j)]^2} \left|\frac{d\theta(H_j)}{dH_j}\right| (j = 1,2,3). \quad (24)$$

The mean value $\langle H_j \rangle$, the variance, $\hat{\sigma}(H_j) = \left(E_2(H_j)\right)^{1/2}$, the third and fourth centered moments ($E_3(H_j)$ *and* $E_4(H_j)$) of the new PDFs given in Eq. (24) can be easily derived using expressions like Eq. (10) with proper changes. Finally, the asymmetry and kurtosis parameters are also derived following Eq. (11) with a proper adaptation.

The asymmetry and kurtosis parameters of the stimuli considered in Table 1 has been computed for the coordinates H_j and are listed in Table 2.

θ_0	σ_θ	$As(H_1)$	$As(H_2)$	$As(H_3)$	$K(H_1)$	$K(H_2)$	$K(H_3)$	$\lvert As(X_i)\rvert$	$\lvert K(X_i)\rvert$
83.8	0.239	-0.1138	0.1138	0.1138	3.0170	3.0170	3.0170	0.1138	3.0170
79.1	0.256	-0.0670	0.0670	0.0670	3.0057	3.0057	3.0057	0.0670	3.0057
79.1	0.230	-0.0602	0.0602	0.0602	3.0046	3.0046	3.0046	0.0602	3.0046
74.1	0.247	-0.0417	0.0417	0.0417	3.0020	3.0020	3.0020	0.0417	3.0020
69.0	0.382	-0.0444	0.0444	0.0444	3.0019	3.0019	3.0019	0.0444	3.0019
68.5	0.304	-0.0341	0.0341	0.0341	3.0011	3.0011	3.0011	0.0341	3.0011
58.4	0.335	-0.0177	0.0177	0.0177	2.9999	2.9999	2.9999	0.0177	2.9999
42.1	0.477	0.0051	-0.0051	-0.0051	2.9989	2.9989	2.9989	0.0051	2.9989

25.1	0.563	0.0491	-0.0491	-0.0491	3.0017	3.0017	3.0017	0.0491	3.0017

Table 2: The first and second columns provide the average angles and standard deviations obtained with filter pair 4/23 ($0^0/90^0$) of group 1A considered in Table 1. The third, fourth and fifth columns provide the values of asymmetry coefficients of the PDFs of the H_j values, and the sixth, seventh and eighth columns provide the values of kurtosis coefficients of the PDFs of the H_j values. The ninth and tenth columns reproduce the absolute values of asymmetry and kurtosis coefficients of the PDFs of the tristimulus values listed in Table 1.

A close inspection of the results of the asymmetry and kurtosis parameters listed in Table 2 indicates that they coincide in absolute values with those obtained for the tristimulus values. This is an expected result, since the transformation from tristimulus values to LMS indicated in Eq. (21) is a linear one, thus the transformed PDFs share their properties. The reason for this behavior is that the Jacobian of the transformation indicated in Eq. (21) is a constant. The values of $H_1 + H_2$ (L+M) shows an identical trend as that shown in Fig. 4.

The way to derive the H_j thresholds closely follows the procedure previously used to obtain the intervals of color-mismatch in tristimulus space with proper adaptations to the current situation. We again use method 2 from Ref. [3] which can be summarized as follows: let $H_{j,L}^{(2)}$ and $H_{j,U}^{(2)}$ be the lower and upper bounds of the interval corresponding to the $H_j (j = 1,2,3)$, i.e., $\hat{I}_j^{(2)} = \left[H_{j,L}^{(2)}, H_{j,U}^{(2)}\right]$. The values for $H_{j,L}^{(2)}$ and $H_{j,U}^{(2)}$ are determined by imposing conditions like those in Eqs. (12) and (13) but the new PDFs $\tilde{g}(H_j)$ are used. We again want to highlight that we do not make any *a priori* assumption concerning the symmetry of the interval $\hat{I}_j^{(2)}$ around $\langle H_j \rangle$. An iterative algorithm is used to determine both $H_{j,L}^{(2)}$ and $H_{j,U}^{(2)}$ and the calculation stops when the tolerance (10^{-8}) is met.

We expect that the intervals of color-mismatch in the LMS space must be asymmetric. The asymmetry can be assessed through the distances from the ends of each interval to the corresponding average value. The distances or thresholds read

$$\Delta H_{j+} = H_{j,U}^{(2)} - \langle H_j \rangle \; (j = 1,2,3),$$
$$\Delta H_{j-} = \langle H_j \rangle - H_{j,L}^{(2)} \; (j = 1,2,3). \qquad (25)$$

Note that the two thresholds given in Eq. (25) are positive, and that the degree of asymmetry is also α-dependent.

The thresholds given by Eq. (25) in the case of α=0.32[0.05] are displayed in Fig. 9(a)[10(a)] for the stimuli considered in Table 2. The ratio between the increment threshold (ΔH_{j+}) and the decrement threshold (ΔH_{j-}) is shown Fig. 9(b)-(d)[10(b)-(d)] for all the color centers of Table II in Ref. [1]. Deviation of the aforementioned ratio from unity indicate the severity of the asymmetry. We can see deviations from symmetry in the range 0.13% in the case of α=0.32 and 10-18% in the case of α=0.05. Deviation from symmetry are in the range of 8.4% in the case of α=0.16 (not shown).

Figure 11 shows the $\log(\Delta H_{3\pm})$ thresholds as a function of $\log(H_3)$ level. The plus thresholds can be described by the following equation

$$\Delta H_{3+} = C(\langle H_3 \rangle + kH_{30}). \qquad (26)$$

A similar equation holds for the minus thresholds. Equation (26) is like the one used in Refs. [11-12]. The value of H_{30} was set to 44.5 Std while parameters C and k were determined using an unconstrained optimization algorithm. The fittings have been made by splitting the data into the three groups of filter pairs. The values of the constants are C=0.019631 and k=0.033709 in the case of α=0.05. They are the same for increment and decrement thresholds. Note that the value of k differs from that reported in Ref. [12]. The

reason for this is that the coefficient a_{33} in Eq. (21) was taken as the unit in Ref. [12]. Note also that the limits of the horizontal axis in Figure are larger than those provided in Fig. 9 of Ref. [12]. Although there is a remarkable closeness of Eq. (26) to the computed thresholds, there appears a large set of color centers whose thresholds are apart from the dashed curve by more than 3 log units. A similar analysis has been conducted for the thresholds determined in the case of α=0.32. The values of the constants in Eq. (26) are C=0.0100504 and k=0.032478. It should be remarked that the scattering of the thresholds obtained in the case of α=0.32 from the curve in Eq. (26) follows a similar pattern as the one shown in Fig. 11 with α=0.05.

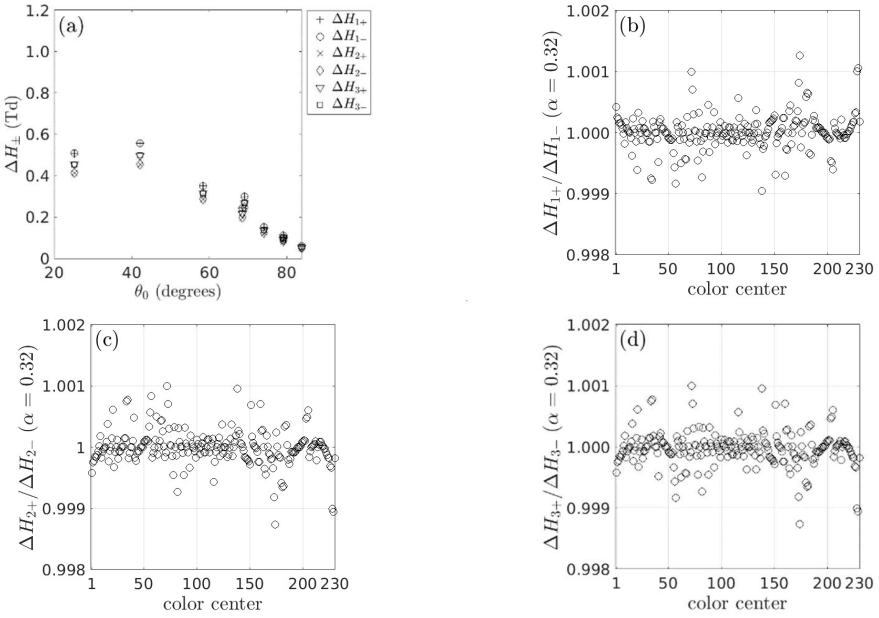

Figure 9: (a) Thresholds of H_j obtained with filter pair 4/23 ($0^0/90^{0)}$ of group 1A. (b)-(d) Ratio between the plus threshold (ΔH_{j+}) and the minus threshold (ΔH_{j-}) for the 230 color centers given in Table II of Ref. [1]. The confidence level is α=0.32.

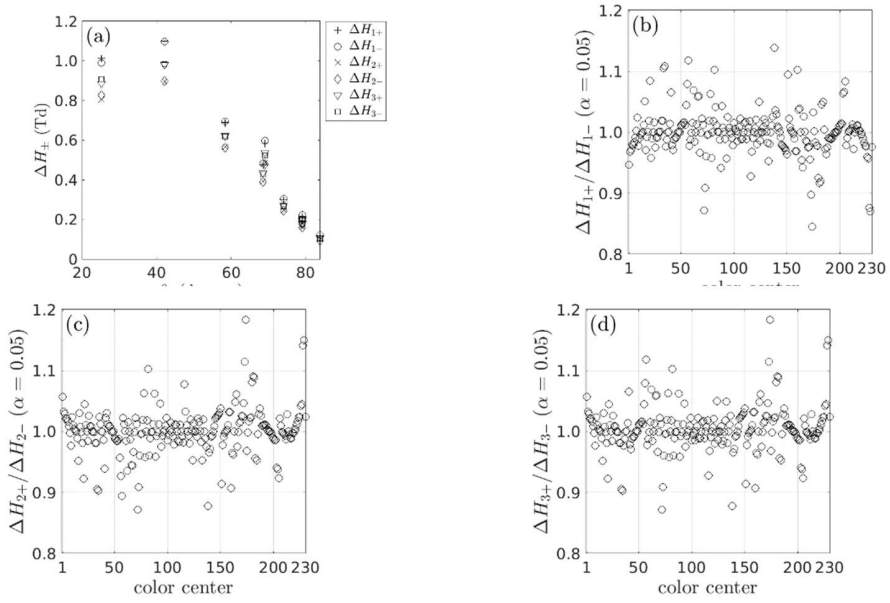

Figure 10: (a) Thresholds of H_j obtained with filter pair 4/23 ($0^0/90^{0)}$ of group 1A. (b)-(d) Ratio between the plus threshold (ΔH_{j+}) and the minus threshold (ΔH_{j-}) for the 230 color centers given in Table II of Ref. [1]. The confidence level is α=0.05.

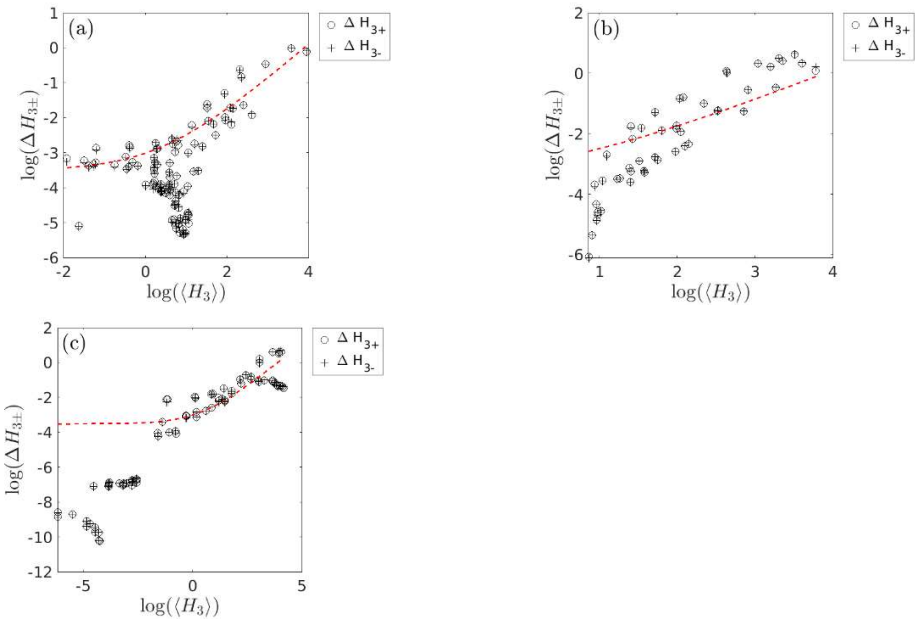

Figure 11: $\Delta H_{3\pm}$ thresholds as function of $\langle H_3 \rangle$ value obtained with group 1A of filter pairs (a), group 1B of filter pairs (b), and group 2 of filter pairs (c). The dashed curve is obtained using the values of C=0.019631 and k=0.033709 in Eq. (26) in the case of α=0.05.

$\Delta H_{1\pm}$ thresholds have also been determined as a function of $H_1 - 2H_2$ value. The results are displayed in Figure 12 in the case of α=0.05. The thresholds reach the smallest values near the zero-excitation level of channel $H_1 - 2H_2$ (chromaticities near unique yellow). Thresholds increase a little when the redness(greenness) of the stimulus increase. The redness(greenness) is associated to positive(negative) values of the excitation level of the channel $H_1 - 2H_2$.

$\Delta H_{1\pm}$ thresholds can be described by the following equation

$$\Delta H_{1\pm} = W\langle H_1 + H_2 \rangle + a\langle H_1 - 2H_2 \rangle \ . \qquad (27)$$

Equation (27) is similar to Eq. (11) in Ref. [12], where the contribution of $\langle H_3 \rangle$ has been neglected. The coefficients W and a in Eq. (27) have determined by fitting the data from group 1A of filter pairs [Fig. 12(a)]. The dashed curves shown in all the panels of Fig. 12 have been obtained using the parameters of the fitting. The greatest discrepancies are obtained for group 1B of filter pairs [Fig. 12(b)], especially for those color centers of the purple region with negative values of $H_1 - 2H_2$. The values of the constants in Eq. (27) are W=0.73325 and a=0.15038 in Eq. (27) in the case of α=0.05, whereas they become W=0.37884 and a=0.075071 in the case of α=0.32.

The reason for the discrepancies found in Figs. 11 and 12 is unclear, but one may speculate that a possible origin of this behavior lies in the fact that tristimulus values of the filters used in Ref. [1] were computed using the CIE1931 color-matching functions, whereas the LMS values were obtained through the modification introduced by Judd.

Let us remind here that the apparatus built in Ref. [1] was designed to produce color stimuli that depend on the angle of the Rochon prism (θ) and the set of tristimulus values of each filter pair $X_{j,u}$ and $X_{j,v}$ (j=1,2,3) as described by Eq. (1). The tristimulus values of the filters used in Ref. [1] were computed as

$$X_{j,A} = K \int_{\lambda 1}^{\lambda f} \hat{x}_j(\lambda)\, p(\lambda)\, T_A(\lambda)\, d\lambda (j = 1,2,3) \ and \ A = u, v. \qquad (28)$$

$T_A(\lambda)$ in Eq. (28) stands for the spectral transmittance of the filter, $p(\lambda)$ is the spectral radiant power distribution of the light source (illuminant A as indicated in the caption of Table I in Ref. [1]), and $\hat{x}_j(\lambda)$ is the j-th color-matching function of the colorimetric observer (CIE1931 standard observer). Finally, K in Eq. (28) is a constant (see Eq. [3(3.3.8)] in Ref. [22]). In using Eq. (28) the author of Ref. [1] implicitly assumed that the spectral transmittance of the rest of optical elements (prisms and lenses) is not wavelength dependent in the spectral range from λ_1 to λ_f. Obviously in the event that the color matching functions of the PGN observer differed from those of the standard observer, the tristimulus values of the color stimuli would be different. This issue cannot be reliably verified with the data available to us.

If we were to use the color-matching functions of Judd and Vos, $\hat{x}_j^{J-V}(\lambda)$, the resulting tristimulus values $X_{j,A}^{J-V}$ will generally differ from $X_{j,A}$.

Transformation matrix in Eq. (21) allows us to obtain LMS tristimulus values assuming that the differences between $X_{j,A}$ and $X_{j,A}^{J-V}$ are negligible. However, note that there are filters with chromaticities in the blue-green region (see Fig. 1) where the differences between $\hat{x}_j(\lambda)$ and $\hat{x}_j^{J-V}(\lambda)$ could play a role, especially in the case of $\hat{x}_3(\lambda)$. Let us consider for example groups 1A and 1B in which one of the filters has a chromaticity close to the white (produced by filter 23). There are certain average angles at which the

other filter of the filter pair provides the greatest contribution to the stimulus to be adjusted in the field of observation, and the effect of using one or the other set of color-matching functions will be more noticeable. Unfortunately, the spectral transmittance of the filters listed in Table I of Ref. [1] remains unpublished so the above discussion is quite speculative.

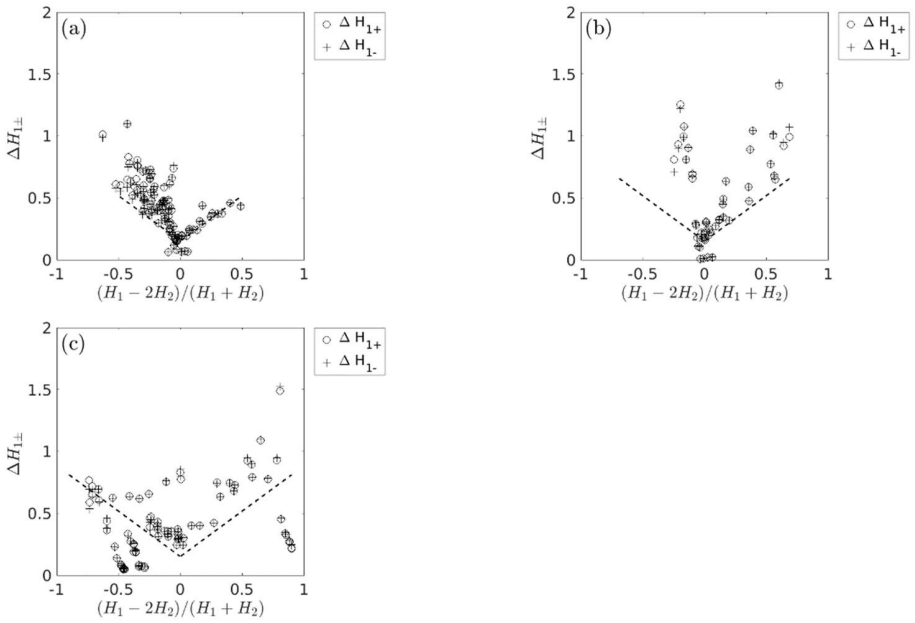

Figure 12: $\Delta H_{1\pm}$ thresholds as function of $H_1 - 2H_2$ value obtained with group 1A of filter pairs (a), group 1B of filter pairs (b), and group 2 of filter pairs (c). The dashed curve is obtained using the values of W=0.73325 and a=0.15038 in Eq. (27) in the case of α=0.05.

The influence of $\langle H_3 \rangle$ value on $\Delta H_{1\pm}$ thresholds has also been analyzed. The results are shown in Fig. 13. We can appreciate that there is no apparent relationship between the two magnitudes. This result is consistent with that shown in Fig. 12 of Ref. [12].

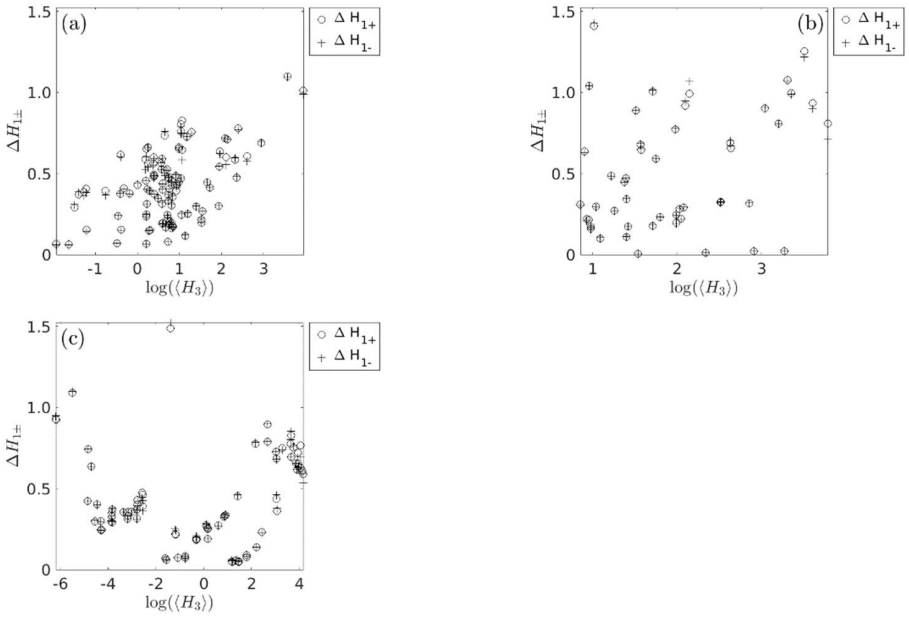

Figure 13: $\Delta H_{1\pm}$ thresholds as function of $\langle H_3 \rangle$ value in log units obtained with group 1A of filter pairs (a), group 1B of filter pairs (b), and group 2 of filter pairs (c) in the case of α=0.05. No systematic relationship appears to exist.

Let us analyze the cone contrast of the three channels. They are obtained by dividing the terms in Eq. (25) by the average value of the corresponding channel. The results are shown in Fig. 14 where the increment cone contrast is plotted as a function of the decrement cone contrast) in the case of α=0.05. A linear relationship exists between them. The slope of the fitting is an indication of the asymmetry, so that the closer it is to one, the smaller the asymmetry. The major departure is obtained for $\langle H_3 \rangle$ where the departure is near to 10%. In the other two channels the departure is lower than 3%. In the case of α=0.32, the slope of the fitting differs from unity in the fourth decimal place for the three channels.

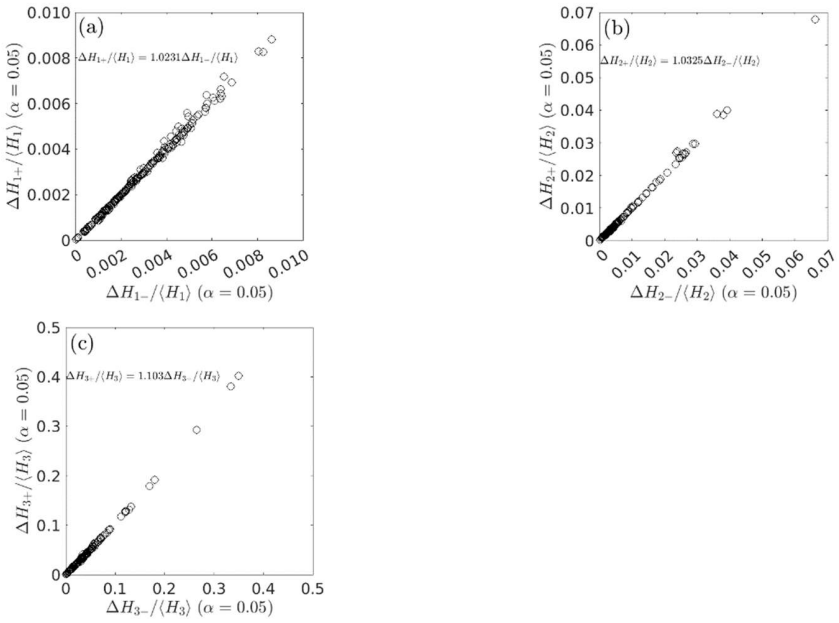

Figure 14: Increment cone contrast versus decrement cone contrast in the case of α=0.05. (a) channel H_1, (a) channel H_2, and (c) channel H_3.

Let us finish this Section by pointing out the question of selecting the transformation matrix in Eq. (21) in terms of the Smith and Pokorny fundamentals. We have repeated the calculations presented in this Section with a different matrix than the one used in Eq (26). This new matrix has the property that it roughly reproduces the Stockman and Sharpe fundamentals [20] adopted by the CIE [21] compared to the fundamentals derived from CIE1931 XYZ values through that matrix [23]. The S-cone(L-cone) thresholds are scattered in a similar way around the fitting curve given by Eq. (26)[(27)]. However, the minimum of L-cone thresholds is not obtained for $\frac{H_1-2H_2}{H_1+H_2} = 0$ (chromaticities near unique yellow) but for $\frac{H_1-2H_2}{H_1+H_2} = -0.47$. This fact is in clear contrast to that obtained in Fig 11 of Ref [12] and led us to keep using the Smith and Pokorny cone fundamentals. The non-availability of raw data of the filters used in Ref. [1] (spectral transmittance) prevents us from carrying out the calculations with the Stockman and Sharpe cone fundamentals.

6 Conclusions

We have derived in this work the interval of color mismatch in chromaticity coordinates using a rigorous statistical analysis. The same technique has been applied to derive the interval of color mismatch in LMS space. The method has been applied to the data provided in Table II of Ref. [1]: the average angles, and the standard deviation of the angle settings. The tristimulus values of the filters were given in Table I of Ref. [1] using the color matching functions of CIE1931 standard observer. Note that deviations of color matching functions of observer PGN from those of CIE1931 standard observer could have an (unknown) impact on the size of the color-mismatch intervals.

We have assumed that the angle settings behave as a Gaussian random process, and we have obtained the PDFs of the chromaticity coordinates. The new PDFs for the chromaticity coordinates deviate from the Gaussian by exhibiting non-null asymmetries, and deviations of the kurtosis parameters from the value of 3 (associated to a Gaussian PDF). Note that although in Ref. [1] no indications about the test of normality of the angle settings were carried out, it seems reasonable to assume it. The PDFs in LMS space share the same properties as the ones obtained for the tristimulus values since a linear transformation is used to go from one space to the other.

Method 2 from Ref. [3] is used to determine the intervals of color mismatch. We assume that the tails of each PDF share the value of the area for a fixed α. The asymmetries of color-differences in chromaticity coordinates become more pronounced for high confidence levels (α<0.32). We conclude that the effect on the color-differences of the changes in luminance can be safely neglected (see Fig. 8). In addition, we have shown that color-differences for α =0.05 cannot be obtained as a simple common scaling factor of the color differences for α=0.32 (see Fig. 7). The asymmetries of LMS thresholds also depend on the confidence level α and become more evident for high confidence levels (α<0.32).

The color difference thresholds $\Delta H_{3\pm}$ as a function of $\langle H_3 \rangle$ in the case of α=0.32 and described by Eq. (26) provide a value for C=0.0100504 very close to the one obtained when analyzing the ellipses in Ref. [1] and reported in Table 1 of Ref. [12] for observer PGN (C=0.010). However, the value for k=0.032478 differs from the one given in Table 1 of by Nagy et al [12] for observer PGN (k=5.53). The reason for this discrepancy is that the coefficient a_{33} in Eq. (21) was taken as the unit in Ref. [12].

The color difference thresholds $\Delta H_{1\pm}$ depend on both the luminance level $(H_1 + H_2)$ and the $H_1 - 2H_2$ value. The values obtained for W and a in Eq. (27) in the case of α=0.32 differ from those listed in Table 2 of Ref. [12] for observer PGN. The reason for this discrepancy remains unclear. However, note that the gamut of chromaticities considered in Ref. [12] for observer PGN is restricted to the 25 color centers corresponding to the ellipses [see Fig. 1(d)] in contrast with the wider scale of chromaticities considered in Table II of Ref. [1] (see Fig. 1(a)-(c) in this work).

$\Delta H_{1\pm}$ thresholds were shown to depend on both the luminance level $(H_1 + H_2)$ and the $H_1 - 2H_2$ excitation level in Refs. [12,13]. The results obtained in this work also fit into current theoretical notions about color vision and the existence of interactions between cone mechanisms. The existence of asymmetries in color matching experiments has also been reported in several experimental works [14]-[20]. In Refs. [17,19] it was shown that identical masking noise has a much greater effect on S-cone increments than S-cone decrements. The results shown in Fig. 14(c) indicate that the major departure from symmetry is obtained for the S-cone channel.

Finally, we want to mention that the level of α=0.05 (95%) selected for the calculations presented in this work is not so high. The detection rate of 82% was used in Refs. [17,19] to determine the parameters of the psychometric function for each stimulus. It corresponds to a value of α=0.18. A similar criterion was adopted in Ref. [15].

Funding No funding has been received to carry out this research.

Acknowledgments The author is grateful to all the people who have participated in the reviewing process of this work for their sharp comments and suggestions. He also acknowledges Universidad Complutense de Madrid for his continuous support.

Disclosures The author declares no conflicts of interest.

Data availability Data underlying the results presented in this paper are not publicly available at this time but may be obtained from the author upon reasonable request.

References

[1] MacAdam DL, "Visual sensitivities to color differences in daylight," J. Opt. Soc. Am. **32**, 247–274 (1942).

[2] Nimeroff I, "Propagation of errors in spectrophotometric colorimetry," J. Opt. Soc. Am. **43**, 531–533 (1953).

[3] Carreño F, "Propagation of errors in a color matching experiment", Col. Res. Appl. DOI: 10.1002/col.22775

[4] Carreño F, Zoido JM, "Statistics of color-matching experimental data," Appl. Opt. **38**, 208–218/col. (1999).

[5] Papoulis A, Pillai SU, *Probability, Random Variables, and Stochastic Processes* (McGraw Hill, Boston, 2002), 4th ed.

[6] Eaton JW, Bateman D, Hauberg S, Wehbring R, *GNU Octave version 4.4.0 manual: a high-level interactive language for numerical computations* (2018).

[7] Wolfram. Inc. "*Mathematica, Version 10.0*". Wolfram. Inc.; 2014.

[8] Brown WRJ, MacAdam DL, "Visual sensitivities to combined chromaticity and luminance differences", J. Opt. Soc. Am. **39**, 808-834 (1949).

[9] Öner, M Kocakoç, İD, "*JMASM 49: a compilation of some popular goodness of fit tests for normal distribution: their algorithms and Matlab codes (MATLAB)*", J. Mod. App. Stat. Meth. **16**, 547-575 (2017).

[10] Smith VC, Pokorny J, "Spectral sensitivities of the foveal cone photopigments between 400 and 500 nm", Vision. Res. **15**, 161-171 (1975).

[11] MacLeod DIA, Boynton RM, "Chromaticity diagram showing cone excitation by stimuli of equal luminance", J. Opt. Soc. Am. **69**, 1183-1186 (1979).

[12] Nagy AL, Eskew RT, Boynton RM, "Analysis of color-matching ellipses in a cone-excitation space", J. Opt. Soc. Am. A **4**, 756-768 (1987).

[13] Boynton RM, Kambe N, "Chromatic difference steps of moderate size measured along theoretically critical axes," Color Res. Appl. 5,13-23 (1980).

[14] Cole GR, Hine T, McIlhagga W, "Detection mechanisms in l-, m-, and s-cone contrast space," J. Opt. Soc. Am. A **10**, 38–51 (1993).

[15] Chaparro A, Stromeyer C, Kronauer R, Eskew R, "Separable red-green and luminance detectors for small flashes," Vision Research **34**, 751–762 (1994).

[16] Vingrys AJ, Mahon LE, "Color and luminance detection and discrimination asymmetries and interactions," Vision Research **38**, 1085–1095 (1998).

[17] Wang Q, Ritchers DP, Eskew RT, "Noise masking of S-cone increments and decrements", J. Vis. **14**, 1-17 (2014).

[18] Shepard TG, Swanson EA, McCarthy CL, Eskew RT, "A model of selective masking in chromatic detection", J. Vis. **16**, 1-17 (2016).

[19] Gabree SH, Shepard TG, Eskew RT, "Asymmetric high-contrast masking in S cone increment and decrement pathways", Vis. Res. **151**, 61-68 (2018).

[20] CIE: Fundamental Chromaticity Diagram with Physiological Axes – Part 1. Technical Report 170-171. Vienna: Central Bureau of the Commission Internationale de l' E´clairage (2006).

[21] Stockman A, Sharpe LT, "Spectral sensitivities of the middle-and long-wavelength sensitive cones derived from measurements in observers of known genotype", Vis. Res. **40**, 1711-1737 (2000).

[22] Wyszecki G, Stiles WS, "Color science: concept and methods, quantitative data and formulae" (John

Wiley & Sons, New York, 1982), 2nd ed.
[23] One of the reviewers of this paper suggested the use of a different matrix in the Eq. (21). This new matrix reproduces quite faithfully the CIE170-1 cone fundamentals compared to the cone fundamentals obtained from the XYZ values through such a matrix.

AUTHOR BIOGRAPHY

Fernando Carreño is an associate professor at the School of Optics and Optometry, Complutense University of Madrid, Spain. He received a PhD degree in holography in 1995. He is a curiosity-driven researcher and his main areas of interest include holography, colorimetry, and physical optics (classical and quantum).